HIGH POWER RADIATION GUIDING SYSTEMS FOR LASER DRIVEN ACCELERATORS

Antonello Cutolo

Istituto Nazionale di Fisica Nucleare - Sezione di Napoli

Dipartimento di Elettronica, Via Claudio 21 80125 Napoli (Italy)

Salvatore Solimeno

Dipartimento di Fisica Nucleare, Struttura della Materia e Fisica Applicata

Mostra d'Oltremare, Padiglione 20 80125 Napoli (Italy)

ABSTRACT

This paper reviews the main problems encountered in the design of an optical system for transmitting high fluence radiation in a laser driven accelerator. Particular attention is devoted to the analysis of mirror and waveguide systems.

I INTRODUCTION

The main conclusions of the workshops held in the last three years and dedicated to laser driven accelerators can be summarized in the fact that, while the performances of the different schemes proposed till now are clear enough, serious doubts have been cast on the possibility of handling efficiently the required high fluence laser beams over distances of the order of a few kilometers [1-3]. This paper is aimed to review critically the wealth of problems connected with the transmission of high power laser beam in a laser driven accelerator (LDA).

The first thing to bear in mind in the design of high power laser systems is the fact that refractive optical components must be excluded wherever possible and, reflective components must be preferred by virtue of their higher optical damage threshold [4]. As an example, we note that in high power lasers the cavity is made of totally reflecting metallic mirrors, the external coupling being ensured by either an unstable configuration or a small hole in one of the mirrors.

An additional reason for excluding refractive lenses wherever possible, is

that they produce large losses due to the transition radiation given off by the fast electrons passing through the lenses.

For the above reasons the choice is limited, as a rule, to one of the following schemes:

1. **Free space propagation**
2. **Mirrors**
3. **Waveguides**
4. **Hybrid configurations**
5. **Self-focusing**

The first four schemes will be carefully analyzed in the next sections. With regard to the self-focusing of the laser beam into the electron bunch [5] proposed by Sessler et al., we limit ourselves to remark that, when it can be efficiently exploited, it seems to be the best approach for solving the problem of the confinement of the radiation in an LDA. However, it is limited by the requirement of high values of the e-beam current intensity.

In conclusion, the main problems we shall deal with are:

1. **Damage threshold**
2. **Coupling of the radiation with the e-beam**
3. **Absorption and diffraction losses**
4. **Manufacturing**

II DAMAGE THRESHOLD IN OPTICAL MATERIALS

Here we give only a short summary of the problems of optical damage, it being assumed that the reader can obtain details from the listed references if desired.

The laser effects induced in optical devices can be either reversible or irreversible. Among the first ones the most important consists in a change of the profile of the surface of the device. These deformations are responsible for the so-called thermally driven abberrations [6]. As they are characteristic of metal surfaces, they will be analyzed in full detail in the next section. Here we prefer to focus our attention on the irreversible damage with reference to dielectric materials, whose importance descends from the fact that a laser beam entering the vacuum chamber of the e-beam, must pass through a transparent window.

In regard to dielectric devices the main possible sources of damage

are melting, thermally induced plastic strains and electric breakdown. The first two classes of damage are characteristic of high average power. In the case of an LDA very high peak intensities (> Gw cm^2) with average intensities less than 1kw/cm^2, are usually required. In these conditions the main mechanism responsible for the damage is simply the electric breakdown.

The problem of an exact definition of the threshold electric field (E_t) for the electric breakdown is quite involved. In fact, while from a theoretical point of view the definition of E_t is straightforward, many experimental factors contribute to prevent the attainment of reproducible values of E_t. Among them, we list the following:

1. Irreproducibility of the temporal and spatial behaviour of the laser field
2. Presence of absorbing inclusions
3. Poor knowledge of the device surface conditions.
4. Self-focusing.

In comparing different experimental results it is customary to define the breakdown threshold as the value at which breakdown occurs in 50% of the pulses. In a well-designed optical system, it is convenient to use electric fields smaller than E_t. In fact, when an electric breakdown occurs a small fraction of the material can be removed from the surface thus generating small irregularities. As pointed out by Bloembergen [7] and Giuliano [8] any kind of surface irregularities as cracks, pores, digs, contribute to reduce the value of E_T. This reduction is a sharp function of the refractive index of the material. As an example, the reduction factor of E_T, due to surface imperfections, is estimated to lie between 2 and 4 for low index materials such as alkali halides, glass and sapphire, while it can be considerably larger in highly refractive materials such as ZnSe and CdTe [7]. This decrease of E_T is not only in inclusion-free materials, where the damage mechanism is electron avalanche breakdown, but also in materials with bulk inclusions, where the damage is due to thermal stresses around the absorbing inclusions.[9]

In general, a good finishing of an optical surface, is obtained by final polishing of the surfaces with ion beams. Fortunately, this results in a marked increase of surface damage threshold compared with that of abrasively polished samples. As an example, we can recall the results obtained by Giuliano,[8] who, after polishing sapphire windows with energetic Ar^+ ion beams, obtained an increase of a factor four in the damage threshold.

The physical mechanism governing optical breakdown in solids is basically the same as in gases. The conduction electrons here play the role of free electrons

and excitation of valence electrons to the conduction bands is essentially equivalent to ionization of atoms in a gas. These features lead to a dependence of the damage threshold on the frequency similar to that of gases excited with microwaves

$$E_T(\omega) \approx E_T(\omega=0)\sqrt{1+\omega^2\tau^2} \qquad (1)$$

where τ is the collision lifetime. In solids τ is estimated to be of the order of 10^{-15} sec[11]. This value of τ gives $\lambda \approx 2\mu m$ for $\omega^2\tau^2 = 1$, which means that, at the wavelengths of pratical interest for LDAS ($\lambda > 1\mu$), E_T is pratically independent of the wavelength and equal to the dc value.

Now, since the breakdown process depends on thermal diffusion (particularly for long-duration pulses) or on plasma growth by electron diffusion from an initial location, we can expect a square root functional form ($\sqrt{\tau_L}$) of the time dependence of the breakdown process (τ_L is the laser pulse length). This leads to predict that the breakdown threshold electric field E_T will scale like $\tau_L^{-1/4}$

In tables I, II, III we have reported some measured values of the damage threshold for different materials with different materials under different irradiation conditions.

Wavelength (μm)	Laser	Transmittance (%)	Damage Threshold
0.694	Ruby	99.0	2.0 G watts/cm^2 in 30 nsec. pulses
0.730	Alexandrite	99.0	1.5 G watts/cm^2 in 100 nsec. pulses
1.053	Nd	99.0	5 joules/cm^2 in 1 nsec. pulses
1.064	YAG	99.0	5 joules/cm^2 in 1 nsec. pulses
1.315	I_2	99.0	5 joules/cm^2 in 1 nsec. pulses

TAB. I Main parameters of windows with antireflection coatings on both sides and working at normal incidence.

Wavelength (μm)	Laser	Reflectance	Damage Threshold
0.694	Ruby	99.6	2 G watts/cm^2 in 30 nsec. pulses
0.730-.790	Alexandrite	99.4	1 G watt/cm^2 in 100 nsec. pulses
1.053-.60	Nd	99.5	5 joules/cm^2 in 1 nsec. pulses
1.064	YAG	99.5	5 joules/cm^2 in 1 nsec. pulses

TAB. II Main properties of some dielectric coated mirrors for 45° incidence.

Wavelength (μm)	Laser	Reflectance	Damage Threshold
0.730-.790	Alexandrite	99.5	2 G watts/cm^2 in 100 nsec. pulses
1.053-.60	Nd	99.5	10 joules/cm^2 in 1 nsec. pulses
1.064	YAG	99.5	10 joules/cm^2 in 1 nsec. pulses
1.315	I_2	99.5	10 joules/cm^2 in 1 nsec. pulses

TAB. III Main parameters of some dielectric coated mirrors for normal incidence

III. METALLIC MIRRORS

A small and well shaped focal spot remains the ultimate goal for a good design of a beam-handling system. The thermal deformations of the mirrors used for focusing on or simply directing a laser beam cause distortions of the wavefronts which result in an increased focal spot. This circumstance reduces the peak irradiance with prejudice for the efficiency and overall performance of the laser apparatus.[12,13]

The reflective optics used in high power laser systems undergo severe thermal cycles when subject to high fluence beams. Even a small percentage of power absorbed can lead to damage and possibly destruction of the mirrors under high power loadings. Although the precautions adopted by the manufacturers are sufficient to prevent destruction, in time the surface of the mirror partially loses its reflectivity because of oxidation. This effect assumes a particular relevance when a laser beam undergoes many reflections, and severe reductions of the power transfer efficiency of the optics may result.

The occurrence of hot spots on the mirrors due to the nonuniform absorption of the oxidized areas may result in a strong deformation of the surface and, consequently, in an aberrated wavefront. This results in an aberration function which depends on the mirror's thermal load. Two classes of aberrations, known as power driven aberrations, can be generally found. One is characterized by low spatial frequencies and is due to the slow intensity variation over the beam diameter. The second class exhibits high spatial frequencies (Fresnel ripples). The presence of these aberrations contrasts with the fact that a small and regularly shaped focal spot is the ultimate goal for a well designed laser beam handling system. All these effects are in general enhanced by the large number of mirrors used for shaping and handling the beams. The control of the exposure cycles of a target to the laser beam requires an exact knowledge of the power falling on it.

We will discuss, now, some analytical results obtained by solving exactly the thermoelastic equations for a water-cooled finite-size mirror illuminated by a c.w. doughnut shaped laser beam. No restrictive hypothesis will be made on the intensity distribution and full account will be taken of the cooling process together with the elastic constraints imposed on the mirror. The mirror will be modelled as a cylinder of finite size (radius R and thickness d) cooled by forced convection as a result of the water flowing at temperature T inside a rigid support to which the inner face of the mirror is stiffly constrained. The thermoelastic

equation will be solved and the results of some numerical calculations will be presented, together with the quantitative evaluation of the influence of the deformations on the peak irradiance.

Consider a metallic mirror (cf. fig.1) exposed on the outer face to a laser beam producing an illumination $I(r,\phi)$. In many cases the beam is collimated and axial-symmetric. We shall ignore temperature transients by considering steady-state distributions. Accordingly, the temperature field inside the mirror $T(r, z, \phi)$ will be found among the solutions of the heat equation

$$\nabla^2 T(r, z, \phi) = 0 \qquad (3.1)$$

subject to the boundary conditions

$$k \frac{\partial}{\partial z} T = A I(r, \phi) = A I_{max} I(r, \phi) \quad \text{for } z = 0 \qquad (3.2a)$$

$$k \frac{\partial}{\partial z} T = h (T - T_c) \quad \text{for } z = -d \qquad (3.2b)$$

$$\frac{\partial}{\partial r} T = 0 \quad \text{for } r = R \qquad (3.2b)$$

with A the absorption coefficient of the mirror (1-5%), k the thermal conductivity ($\sim$380 W/m for copper), h the thermal convection coefficient ($10^2 \div 10^4$ W/m^2 °C) and T_c the temperature of the cooling water. By the variable separation technique we get the results plotted in fig.2 [4,12].

The temperature field $T(r, z, \phi)$ induces a deformation of the mirror described by a displacement vector $u(r, z, \phi)$. Assuming an axial symmetry the thermoelastic equation can be solved to give the results plotted in fig. 3 [12].

The effect of the thermal deformation on the focusing properties of the mirror can be summarized in the function I/I*, where I is the peak intensity in the focus of our mirror when the deformations of its surface are taken into the right account while I* is the same intensity when these deformations are absent.

In fig. 4 we have plotted the thermal coefficient h as a function of the cooling water flow rate while I/I* is plotted in fig. 5 as a function of the thermal coefficient h.

Oxide films, presumibly cuprous oxide,form as a rule on copper after exposure to air. This explains the spread of the optical reflectivity values measured by several authors (see table IV). According to Roberts [15] the absorption

coefficient attains its lowest value (0.7%) for a copper specimen thoroughly annealed in hydrogen, electropolished to produce a finished surface, and made clean by heating it to 277°C in a vacuum chamber at a pressure of less than 10^{-5} mm. The other listed values refer to specimens exposed to the atmosphere. The absorption coefficient A ≈ 1.3%, measured with the technique of ref.16, for a Spawr mirror LCuW-081 having a diameter of 5 inches and a guaranteed reflectivity higher than 99% (at delivery)[16] is slightly higher than the above referred values.

Table II reports some measurements carried out on some steel SAE 1045 samples irradiated with a 500 W CO_2 laser delivering about 250 watts.

Then a polished steel sample exposed to the atmosphere almost twice as much as a film of pure iron evaporated on a substrate at a pressure of about 10^{-6} mm. This confirms the importance of the oxide films forming on the surface of metallic specimens exposed to air as already discussed for the copper mirrors.

TABLE IV OPTICAL DATA FOR SEVERAL COPPER SAMPLES

Author	Ref.	$k'^{(a)}$	$k''^{(a)}$	$n^{(b)}$	$k^{(b)}$	$100(1-R)^{(c)}$
Beattie et al.	19	-2500	750	7.422	50.52	1.13
Shkliarevskii	20	-3406	1248	10.96	59.22	1.20
Roberts						
(bare copper)	15	-5274	1386	9.46	73.24	0.69
(same with						
40 Ä film)	21	-3988	902	7.09	63.54	0.69
Spawr et al.						
(Spawr mirror						
LCuW-081)	16					0.8

a) k'ik" is the relative dielectric constant

b) n + ik indicates the complex refractive index

c) R represents the reflectance

TABLE V ABSORPTION COEFFICIENTS OF SOME SAE 1045 STEEL SAMPLES WITH DIFFERENT SURFACE CONDITIONS AND FINISHING.*

Surface Condition	Incident Power (W)	Absorbed Power (W)	Absorption Coefficient
Polished	257	29	0.11
Blasted	257	88	0.34
As it is	257	95	0.37
Blackened	257	132	0.51
Phosphate Coated	257	239	0.93

* Chemical composition, % in weight: 0.45 C; 0.8 Mn, 0.3 si, 0.1 Cr, 0.02 S

IV METALLIC AND DIELECTRIC COATED WAVEGUIDES

A number of metallic waveguides have been studied [21] in the search for flexible systems able to deliver the output of CO_2 lasers. All these devices, the best understood being rectangular, helical and circular waveguides [22, 23], share the feature of transmitting efficiently the low-order modes only. This circumstance, together with the fact that their dimensions (height for rectangular guides or curvature radii for the helical and circular ones) are many wavelengths large, limit the divergence of the delivered beams. Reciprocally, the alignment and the matching of an incoming beam with the geometry of the guide input section are very critical. These features have been limiting factors in using these devices in laser metal-working system[4].

In more recent years, various types of midinfrared optical fibers have been developed. Reports have been given of $ZnCl_2$ glass fiber and of polycristalline and single crystal of thallium and silver halides.[24, 25] Hidaka et al [26] have also proposed a new type of fiber in which oxide glass is used as the cladding material to define a hollow core. Some of these structures are currently employed in hollow waveguide lasers[26].

As an outgrowth of these developments, it is interesting to analyze structures combining the main characteristics of metallic and hollow dielectric waveguides, that is ruggedness and low losses. Some authors [28] have studied the propagation characteristics of circular waveguides with dielectric load for increasing the bandwidth of a gyratron. In their analysis they did not account for the finite resistivity of the metals, which becomes an important factor in the midinfrared. In addition, the coating thickness was much smaller than a wavelength. So they did not point out at some special features of these structures occurring when the optical thickness of the coating assumes values close to odd multiples of $\pi/2$.

Coated guiding structures can be made by depositing a dielectric film on metallic strips cut to form the top and the bottom walls of the waveguide.

In this section we are going to review the main properties of both metallic [29] and dielectric coated waveguides [30] for high power laser transmission [31].

With reference to the geometry illustrated in fig. 6 we can express the mode function $u(x, z) = E_y(H_y)$ relative to a TE(TM) mode in the form [30]

$$u = e^{i(\beta+i\alpha)z} \begin{cases} \left\{ \begin{matrix} \cos \\ \sin \end{matrix} \right\} (K_x X), & |x| < b \\ A_+ \left\{ \begin{matrix} \cos \\ \sin \end{matrix} \right\} (K_{x1} X + \phi_+) + A_- \left\{ \begin{matrix} \cos \\ \sin \end{matrix} \right\} (K_{x1} + \phi_-) & \\ b < |x| < b + \delta & \end{cases} \tag{2}$$

where a time dependence $\exp(-i\omega t)$ is understood and suppressed and k_x and k_{x1} satisfy the dispersion relations

$$K_x^2 + (\beta + i\alpha) = K^2 \tag{3}$$

and

$$K_{x1}^2 + (\beta + i\alpha) = n_1^2 k^2,$$

n_1 being the generally complex refractive index of the coating and $k = \omega/c$ the wavenumber. The two boundary matching conditions can be both satisfied if k_{x1} and k_x comply with the eigenvalue equation for the transverse propagation constants

$$K_x \tan\left(K_x b + (m-1)\pi/2\right) = \begin{cases} -\left(n_1^2/K_{x1}\right) \tan\left(K_{x1} + \psi\right) & \text{TM modes} \\ K_{x1} / \tan\left(K_{x1} + \psi\right) & \text{TE modes} \end{cases} \tag{4}$$

with $m > 0$ integer, and

$$\psi = \begin{cases} \tan^{-1}\left(i K_{x1} \tilde{n}_2 / K\right) & \text{TM modes} \\ \tan^{-1}\left(i K_{x1} / \tilde{n}_2 k\right) & \text{TE modes} \end{cases} \tag{5}$$

Equation (4) has been solved numerically with respect to k_x and plots of $\mathrm{Re}(k_x b)$ and $\mathrm{Im}(k_x b)$ for the TE_{01}, TE_{02}, TE_{03} modes are presented in fig.7 for $n_1 = 3$, $\tilde{n}_2 = i60$ (full lines), $\tilde{n}_2 = 7 + i60$ (dotted lines) and $kb \approx 150$ ($b = 0.25$ mm at $\lambda = 10\,\mu$m). Notice that $\tilde{n}_2 = 7 + i60$ is the complex refractive index of copper surfaces at $10\,\mu$m.

The loss factor α_m^{TE} of the mth TE mode can be calculated by solving the eigenvalue equation (4) for the transverse propagation constant, by taking into account the imaginary part of n_1 and the real (β) and imaginary (α) components of k_z. Following Nishihara et al. [32] we can use the reflection coefficient r_{TE} of the dielectric coated metallic surface for an incidence angle $\phi_0 = \sin^{-1}(k_x/k)$

$$\varrho_{TE} = \left[1 - \frac{k_x}{n_e k} - i \left(\frac{k_{x1}}{\tilde{n}_e k} - \frac{k_x}{k_{x1}} \right) \tan \left(k_{x1} \delta \right) \right]$$

$$\cdot \left[1 + \frac{k_x}{n_e k} - i \left(\frac{k_{x1}}{\tilde{n}_e k} + \frac{k_x}{k_{x1}} \right) \tan \left(k_{x1} \delta \right) \right]^{-1} \qquad (6)$$

to calculate α_{TE}

$$\alpha_{TE} = - k_x \left(\ln |\varrho_{TE}| \right) / 2 kb \qquad (7)$$

Equation (7) holds true for values of the dielectric thickness far from the transition regions, where the eigenvalue equation (eq.(4)) must be solved numerically. Figure 3 shows the loss α_{TE} for a metallic waveguide with kb = 150 and loaded with a dielectric film with n_1 = 1.5,3.

The radiation pattern and the coupling of a cylindrical gaussian beam into the uncoated metallic waveguide modes have been calculated by many authors (see e.g. refs.21,32) by assuming the field on the open end coincident with the mode itself. This corresponds to neglecting the reflection caused by the waveguide truncation. While this assumption is in practice correct for metallic waveguides, the same does not hold true when there is a coating. In fact, in this case a surface wave can be excited, which, travelling backward inside the dielectric substrate, can detract power from the forward scattered wave. In this case the analysis of the diffraction at an open end is a very difficult problem, which can be approximately solved by assimilating the waveguide walls to a half-plane with two face impedances defined, as usual, by $Z_s = E_y / H_z$.

Relying on the method proposed by Maliunzhinets [33] the following expression on the field diffracted by the dielectric coated waveguide has been obtained in ref. 30

$$v_d (\rho, \phi) = - \frac{\exp (ik\rho + i\pi/4)}{(2\pi\rho/b)^{1/2}} \exp (i\phi) \frac{\operatorname{sinc}(\phi + \phi_o) + \operatorname{sinc}(\phi - \phi_o)}{\sin \phi_o + i (\phi/\phi_o) \cos \phi_o} \qquad (8a)$$

where

$$\phi_o = kb \sin \phi_o = k_x^{(m)} b, \quad \phi = kb \sin \phi \qquad (8b)$$

Now, taking advantage of the reciprocity theorem the coupling effieciency F_m (defined as the ratio between the power coupled into the mth mode and power of the input beam) can be easily calculated [30] thus giving the results plotted in fig.9.

Now, it is worth discussing briefly some problems relevant to the manufacture of these waveguides. As in high efficiency LDA the laser beam must be kept well focused over distances of several hundred metres, we believe that dielectric coated waveguides would not be the best choice. In fact, the thickness of the dielectric coating should be controlled with a very high precision to avoid the mode coupling, which could easily reduce the coupling efficiency between the radiation and the e-bunch.

After these considerations a metallic waveguide seems to be the best choice and so in the next part of this section we shall focus our attention on these devices. We start by analyzing the loss factor α_m (m being the index of the mode) by a simple ray-optical analysis. In fact, a mode TE_{mo} or TM_{mo} is formed by two plane waves travelling at angle $\vartheta_m = \lambda m \pi / 2a$ with respect to the waveguide axis. Then, each ray travels a distance $d_m = a/\tan\vartheta_m$ between two reflections on upper and lower plates. Let $A(\vartheta)$ the loss per reflection at the incidence angle $i = \pi/2 - \vartheta_m$, the mode undergoes an attenuation per unit length equal to

$$\alpha_m = \frac{m \lambda A(\vartheta)}{2 a^2} \tag{9}$$

A being the absorptance of the metal at the grazing angle ϑ.

For grazing incidence $A(\vartheta)$ is given by (see f.i. Ref.17):

$$A^{TE}(\vartheta) = 4 Re\left(n^{-1}\right) \sin\vartheta \cong 4\vartheta Re\left(n^{-1}\right), \tag{10a}$$

$$A^{TM}(\vartheta) = \frac{4 Re(n) \sin\vartheta}{1 + 2 Re(n) \sin\vartheta + |n^2| \sin\vartheta} \tag{10b}$$

n being the generally complex refractive index of the metal. Consequently,

$$\alpha_m^{TE} \sim \frac{m^2 \lambda^2}{a^3} Re\left(n^{-1}\right), \quad \alpha_m^{TM} \sim \frac{m^2 \lambda^2}{a^3} Re(n) \tag{11}$$

A transmission of more than 95% per meter in a straight aluminium waveguide having a cross section of 0.5 x 7 mm has been measured at $\lambda = 10\mu$.

It is noteworthy that α^{TE} scales with the inverse cubic power of the waveguide height. Consequently, using a waveguide 5 mm high the attenuation reduces to $5 \times 10^{-5}\ m^{-1}$.

Another factor to be considered is the ratio between the electric fields on the walls and in the middle of the waveguide for the TE_{10} mode, which exhibits the

lowest losses,

$$\frac{E_{wall}}{E_{centre}} = \frac{1}{2}|A| = \frac{1}{2} 4 Re\left(n^{-1}\right)\frac{\pi\lambda}{2a} = \frac{\pi\lambda}{a} Re\left(n^{-1}\right) \qquad (12)$$

Since n oscillates between 60 and 70 for Al, Cu or Au, the above ratio is of the order of:

$$\frac{E_{wall}}{E_{centre}} \sim \frac{0.5 \cdot 10^{-3}}{a} \qquad (13)$$

with "a" expressed in mm. With a spacing of a few millimeters the field on the walls reduces to $10^{-3} \div 10^{-4}$ of the value in the middle. This reduction is of the same order of magnitude as the reduction which can be reasonably achieved in a hollow dielectric waveguide.

If we assume that E_{centre} can reach values of the order of a few GV/m, a rough estimate of the field inside the metal yields $E_{metal} \sim$ MV/m. This field corresponds to a flux density of $\sim 10^5$ W/cm^2. The same intensity can be reached by illuminating the metal almost at normal incidence with a flux density of $\sim$10 Mw/cm^2, having assumed a reflectivity a 99 ÷ 98%. Good quality copper mirrors can withstand such high flux densities for a few nanoseconds.

If we illuminate a metallic waveguide with a well focused beam, we can excite a few modes in such a way as to keep the field on the walls below the damage threshold value. This means that the most critical stage of this system is represented by the coupling of the input beam with the waveguide.

In case of Gaussian beams, the percentage of the power channeled through any waveguide mode can be calculated by assimilating the beam to that irradiated by a source located at a complex point. In so doing it is possible to apply the geometrical theory of diffraction (GTD) which can account very accurately for the geometry of the metal [29]. In fig.10 we have plotted the coupling coefficients for different parameters of a Gaussian beam. These plots show how critical the coupling with these structures is.

The reader is justified in questioning how well founded is the suggestion of using dielectric or metallic waveguides for confining and guiding the very powerful laser beams required by laser accelerators, over distances of some hundred meters. Inquiry of the laser damage literature to date indicates that wide-bandgap insulators can withstand rms optical electric fields ranging from 1 MV/cm to 10 MV/cm depending on the pulse duration. These field breakdown thresholds correspond

to flux densities of $10^{-3} \div 10^{-1}$ Tw/cm^2.

The experimental data refer to the case of normal incidence. In case of grazing incidence we can expect a notable increase of the damage threshold. If we assume that the damage originates in the bulk of the dielectric the above quoted values of electric field will modify as

$$\frac{E_{normal}}{E_{grazing}} = \left(\frac{T_{graz}}{T_{nor}}\right)^{1/2} \tag{14}$$

where $T_{nor} = 4n(n+1)^2$ is the transmission coefficient for normal incidence while T_{graz} refers to the case of grazing incidence.

For optical quality surfaces satisfying Fresnel's equations of the reflectivity we have at grazing incidence

$$T^{TE} = \frac{4\vartheta}{n} \quad , \quad T^{TM} = 4\vartheta n \tag{15}$$

so that

$$\begin{aligned} E_{threshold} &\sim \vartheta^{-1/2}\,(1 \div 10) \ \text{MV/cm} \quad (TE) \\ &\sim \frac{\vartheta^{-1/2}}{n+1}\,(1 \div 10) \ \text{MV/cm} \quad (TM) \end{aligned} \tag{16}$$

If we assume that our dielectric waveguide is used to confine a gaussian beam having a spot size ω_o, we obtain a rough estimate of the incidence angle in the above relation by equating ϑ to the far field aperture, i.e.

$$\vartheta \sim \frac{\pi\lambda}{\omega_o} \tag{17}$$

being the waist spot size. Accordingly,

$$E_{threshold} \sim \left(\frac{\omega_o}{\pi\lambda}\right)^{1/2}(1 \div 10) \ \text{MV/cm} \tag{18}$$

If we consider that the field on the wall is equal to that on the axis times $\exp(-a^2/w^2)$, we obtain a rough estimate of the highest rms field obtainable in the centre of a hollow dielectric waveguide

$$E_{max} \sim \left(\frac{\omega_0}{\pi\lambda}\right)^{1/2} e^{a^2/\omega_0^2} \quad (1 \div 10) \quad MV/cm \tag{19}$$

As an example, if we choose a = 1.5 mm, λ = 10.6 μm, we obtain

$$E_{max} \sim 8 \div 80 \quad GV/m \tag{20}$$

These values are of the correct order of magnitude compared to laser fields considered for acceleration where useful gradients of 0.1 ÷ 1 GeV/m, are assumed.

Figure 10 shows that the coupling is a very sharp function of the orientation and of the parameters of the laser beam. Unfortunately, flared waveguides as well as compound parabolic concentrators [31] cannot be used in our case. This is due to the fact that they increase the coupling efficiency between the input laser beam and the waveguide, but the coupled power is shared between several modes thus reducing the acceleration gradient.

ACKNOWLEDGEMENTS

Useful discussions with Dr. A. Renieri and Dr. M. Placidi and the assistance of Mrs F. Candiglioti are sincerely acknowledged.

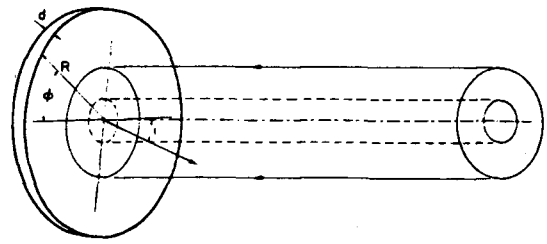

Fig. 1 The metallic mirror in its reference system

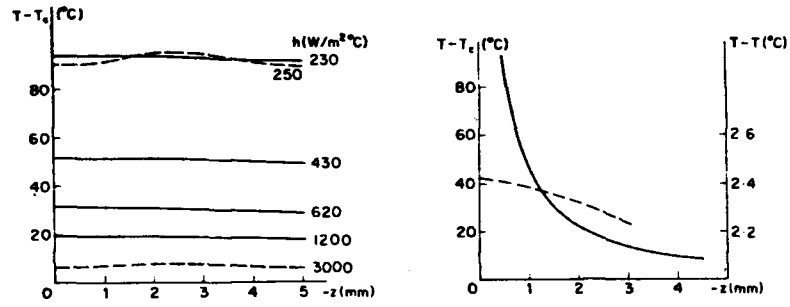

Fig. 2 Plot of the temperature T-Tc (Tc is the reference temperature set equal to zero in our calcolations) of the exposed face of the mirror with R = 10 cm, d = 5 mm, A = 0.05 for different value of h and k = 384 W/m °C (copper, continous lines) and k= 3.84 W/m °C (dotted lines). An incident laser beam with a continous power of 10 Kw has been assumed (after ref. 12).

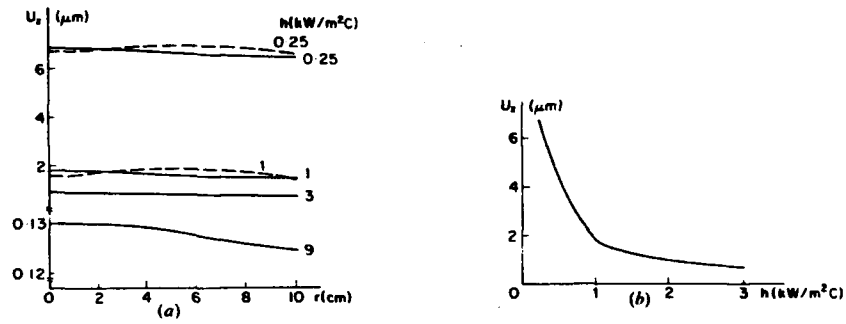

Fig. 3 Normal displacement of the exposed face of the mirror described in fig. 2 (on the top) and of the centre of the same exposed face (on the bottom).

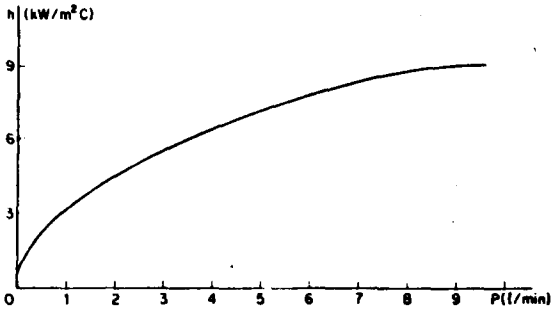

Fig. 4 Plot of the thermal coefficient h as a function of the flow rate of the cooling water.

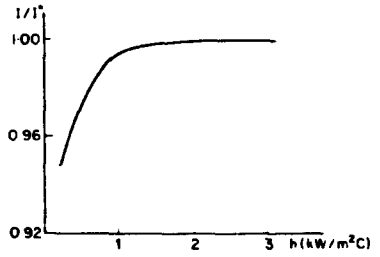

Fig. 5 The ratio I/I^* versus the thermal coefficient h.

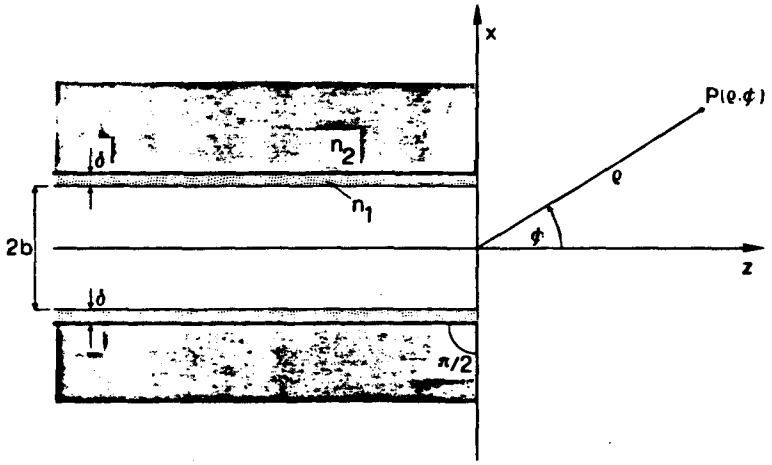

Fig. 6 The dielectric coated metallic waveguide.

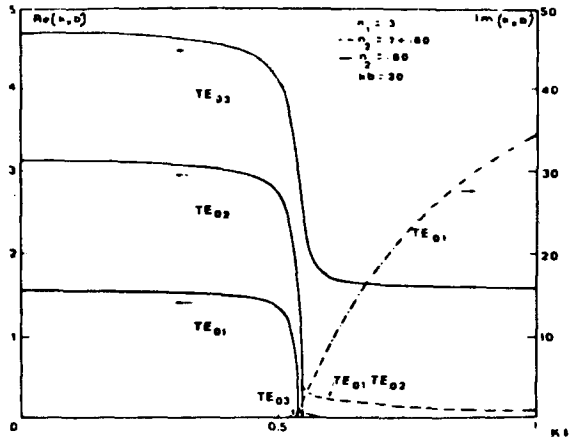

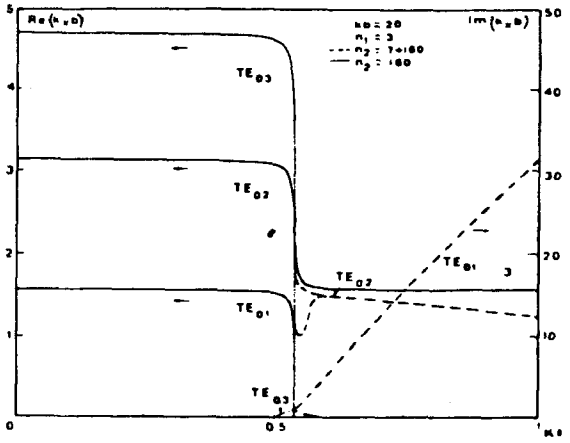

Fig. 7 Plots of $Re(k_x b)$ and $Im(k_x b)$ for TE_{01}, TE_{02}, TE_{03} modes versus $k\delta$ for a waveguide with kb = 20 (fig.7a) and kb = 150 (fig.7b). In both cases $n_1 = 3$ and $\tilde{n}_2 = i60$ (___) and $\tilde{n}_2 = 7 + i60$ (---).

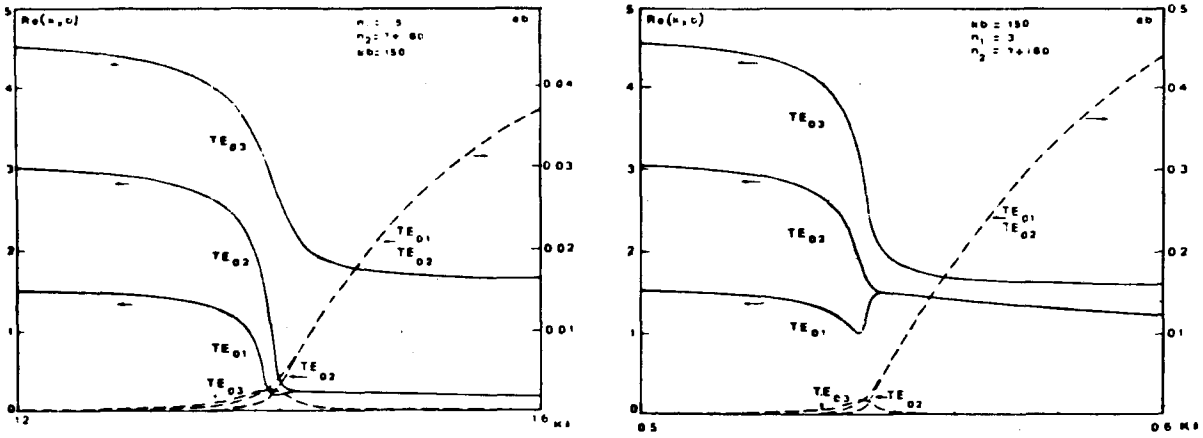

Fig. 8 Plots of $Re(k_x b)$(full lines) and the loss factor α (dotted lines) for the TE_{01}, TE_{02}, TE_{03} modes of the waveguide with kb = 150 and $\tilde{n}_2 = 7 + i60$, $n_1 = 1.5$ (fig.8a) and $n_1 = 3$ (fig.8b).

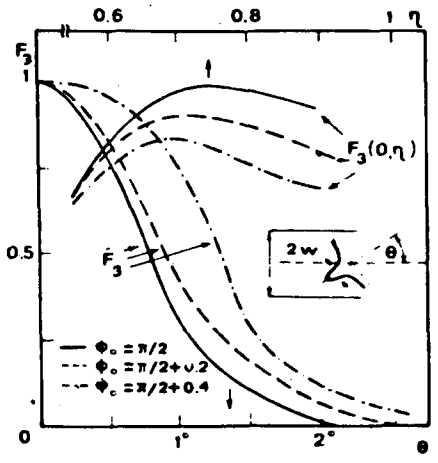

Fig. 9 Coupling efficiency $F_3(0, \eta)$ of a cylindrical gaussian beam versus $\eta = w/b$ and $F_3 = F_3(\theta, \eta_{opt})/F_3(0, \eta_{opt})$ for different values of Φ_0. Θ is the angle between the waveguide and the laser beam axis. Note that the dielectric coating decrease the sensitivity of the coupling efficiency to the alignment.

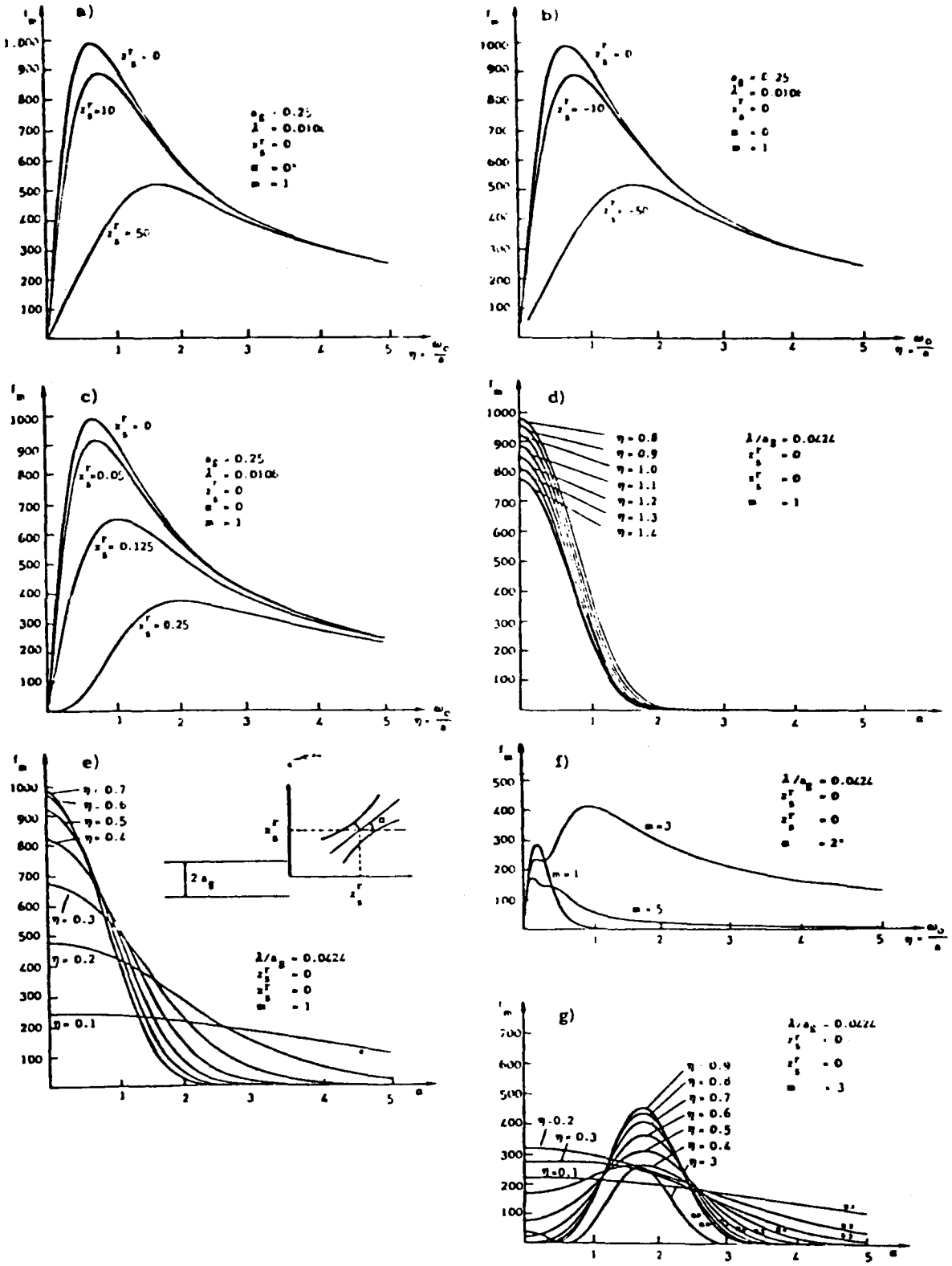

Fig. 10 Coupling coefficient of a Gaussian beam with the fundamental (m = 1) and third (m = 3) modes of a metallic waveguide as a function of $\eta = w_o/a$, and the coordinates x_s^r, z_s^r, of the waist, α the angle formed by the propagation axis of the beam with the waveguide.

REFERENCES

1. P.J. Channel Ed., Laser acceleration of particles AIP (N.Y. 1982)
2. The Challenge of Ultra High Energies, Proc. of the ECFA-RAL meeting, Oxford (1982)
3. These proceedings
4. V. Bartiromo, A. Cutolo, S. Solimeno in "Laser Matter Interaction" ed. by M. Bertolotti, Plenum Press (1984)
5. A. Sessler, these proceedings
6. P.V. Avizonis in "Adaptive Optics and short wavelength sources" eds. S.F. Jacobs, M. Sargent III and M.O. Scully, Addison Wesley (1978)
7. N. Bloembergen, Appl. Opt. 12, 661 (1973)
8. C. Giuliano, Appl. Phis. Lett., 21, 39 (1972)
9. N. Bloembergen, IEEE J. of Quant. Electron., QE-10, 375 (1979)
10. Shen, The principles of non-linear Optics, J. Wiley and Sons, N.Y. 1983
11. S.A. Ramsden, W.E.R. Davis, Phis. Rev. Lett. 13, 227 (1964)
12. A. Cutolo, P. Gay, S. Solimeno, Optica Acta 27, 1105 (1980)
13. A. Cutolo, Alta Frequenza, LXIX, 261 (1980)
14. F. Crescenzi, A. Cutolo, P. Gay, S. Solimeno, Opt. Engeneering 21, 511 (1982)
15. S. Roberts, Phys. Rev. 118, 1509 (1960)
16. W.J. Spawr, R. Pierce, SPAWR Opt. Res.; Rept. 74-004 (1976)
17. Landolt, Börstein, Eigenschaften der Materie in Ihren Aggregatzustanden, 8. teil, Springer Verlag; Berlin (1962)
18. F. Bueche, J. Opt. Soc. of 38, 806 (1948)
19. J.R. Beattle, C.K. Conn, Phylos Mag. 46, 989 (1955)
20. I.N. Shkharevskii, V.G. Padalka, Opt. Spektrosk. 6, 78 (195
21. E. Garmire, T. McMahon and M. Bass, IEEE J. Quant. Electron. QE-16 (1980) 23
22. L. Casperson, IEEE Quant. Electron. QE-15 (1979) 491
23. H. Krammer, Appl.Optics 17 (1978) 316
24. S. Sakuragi, M. Saito, Y. Cubo, K. Imagawa, H. Kotami, T. Marikawa and J. Shimada, Optics Lett. 6 (1981) 629
25. T.J. Bridges, J.S. Hasiak and A.R. Struad, Optics Lett. 5 (1980) 85
26. R.L. Abrams, and W.B. Bridges, IEEE J. Quant. Electron. Q9 (1973) 940
27. T. Hidaka, T. Marikawa and J. Shimada, J. Appl. Phys. 52 (1981) 4467
28. S.Y. Choe, H.S. Ulm and S.A. Chu, J. Appl. Phys. 52 (1981) 4508
29. F. Crescenzi, P. Gay, A. Cutolo, I. Pinto, S. Solimeno, Proc. of 1980 Europ. Conf. on Opt. Systems, SPIE vol. 236, 365 (1981)
30. A. Cutolo, S. Solimeno, Opt. Comm. 43, 323 (1982)
31. S. Solimeno, in ref. 1
32. K.D. Laakmann, W.H. Steier, Appl. Opt. 15, 1334 (1976)
33. G.D. Malinzhiuets, Soviet Phys. Dokl. 3, 752 (1958)

Discussion

R. Evans, RAL

I have a question concerning the maximum intensity in the waveguide mode. The number quoted was 80 GV/m. Is that experimentally measured or is it a theoretical limit?

Answer

It is an extrapolation depending on how the damage threshold varies with the pulse length. It should be possible for pulses with a length between 5, 10, or at the most 50 ps. For longer pulses this damage threshold goes down inversely proportional to the square root of the pulse length.

H. Lengeler, CERN

An experimental value given to me by K. Witte is about 1 GV/m for a 1 ns single-shot pulse, at 10 μm.